格子QCDによるハドロン間相互作用

with HAL QCD Collaboration

高密度中性子物質と冷却原子気体

with **前田賢志（東大・理）**、G. Baym（UIUC)

初田哲男

理論研究部門　仁科加速器研究センター

理化学研究所

Phase Diagram @ 1980

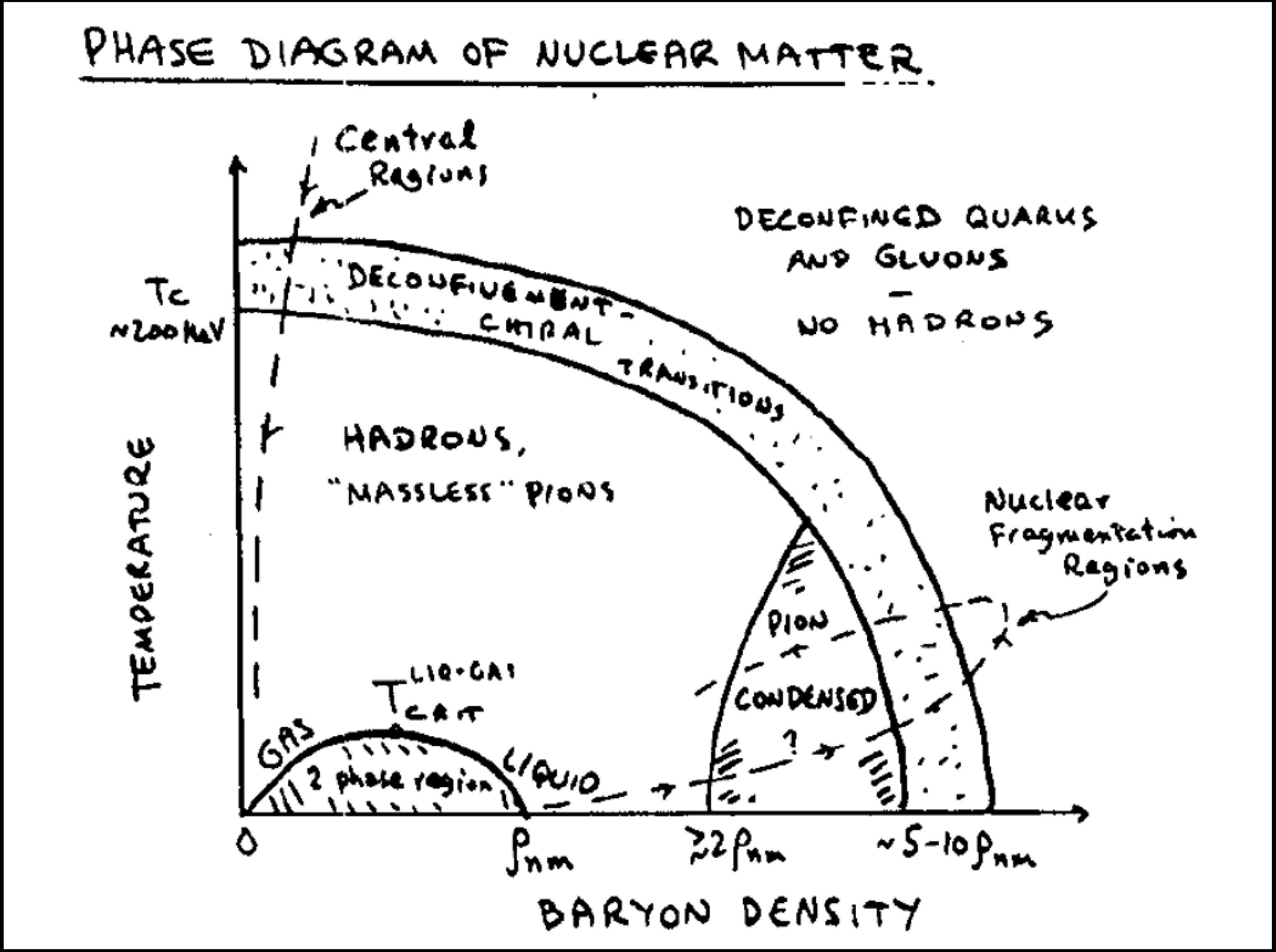

G. Baym (1980)

Phase Diagram @ 2011

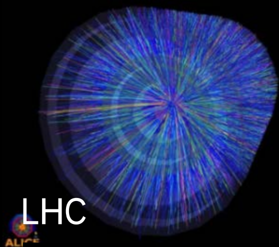

LHC

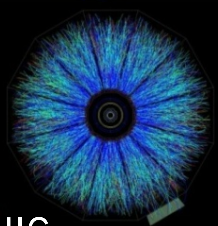

RHIC

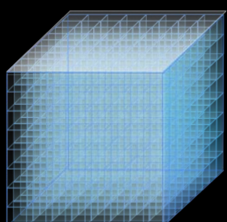

Lattice QCD

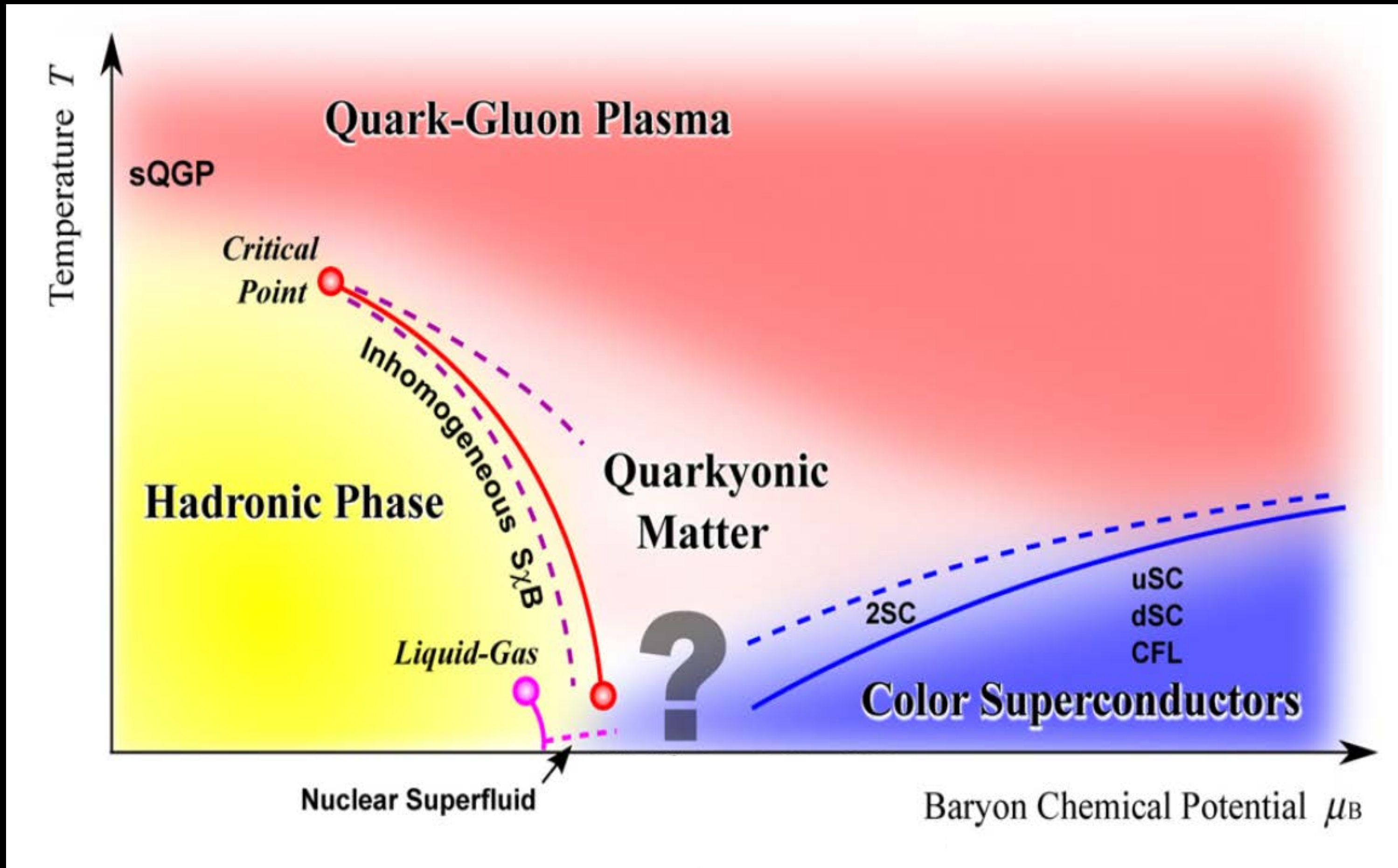

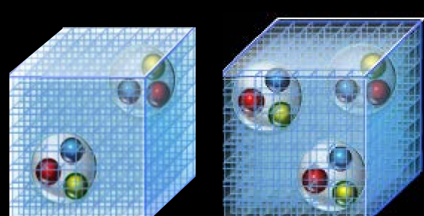

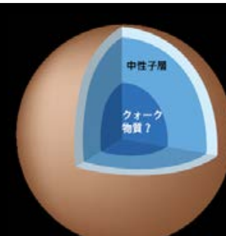

K. Fukushima and T. Hatsuda,
“The Phase Diagram of Dense QCD”
Rep. Prog. Phys. 74 (2011) 014001

高密度物質の理解へむけて

1. 有限密度格子QCD計算
   - 最善の策
   - 負符号問題のためμ/T > 1では困難

2. QCDに基づくBB, BBB相互作用 (京コンピューター)
   → 従来の多体問題手法 → ハイペロン物質 with BBB相互作用
   - 次善の策： ハイペロンは完全に入る
   - ４体力、５体力、...？ クォーク物質への相転移？

3. (低エネルギー) 重イオン衝突実験
   - 数倍の原子核密度
   - 温度も上がる

4. 中性子星観測, マグネター観測
   - M-R 関係、冷却曲線： X線、磁場、重力波

5. 実験室で類似系（冷却原子分子気体）
   - 低密度中性子物質 ⇔ 2成分フェルミ原子気体
   - 中間子凝縮 ⇔ 双極フェルミ原子気体
   - ハドロン-クォーク相転移 ⇔ ３成分フェルミ原子気体、ボース・フェルミ原子混合気体

http://www.jicfus.jp/field5

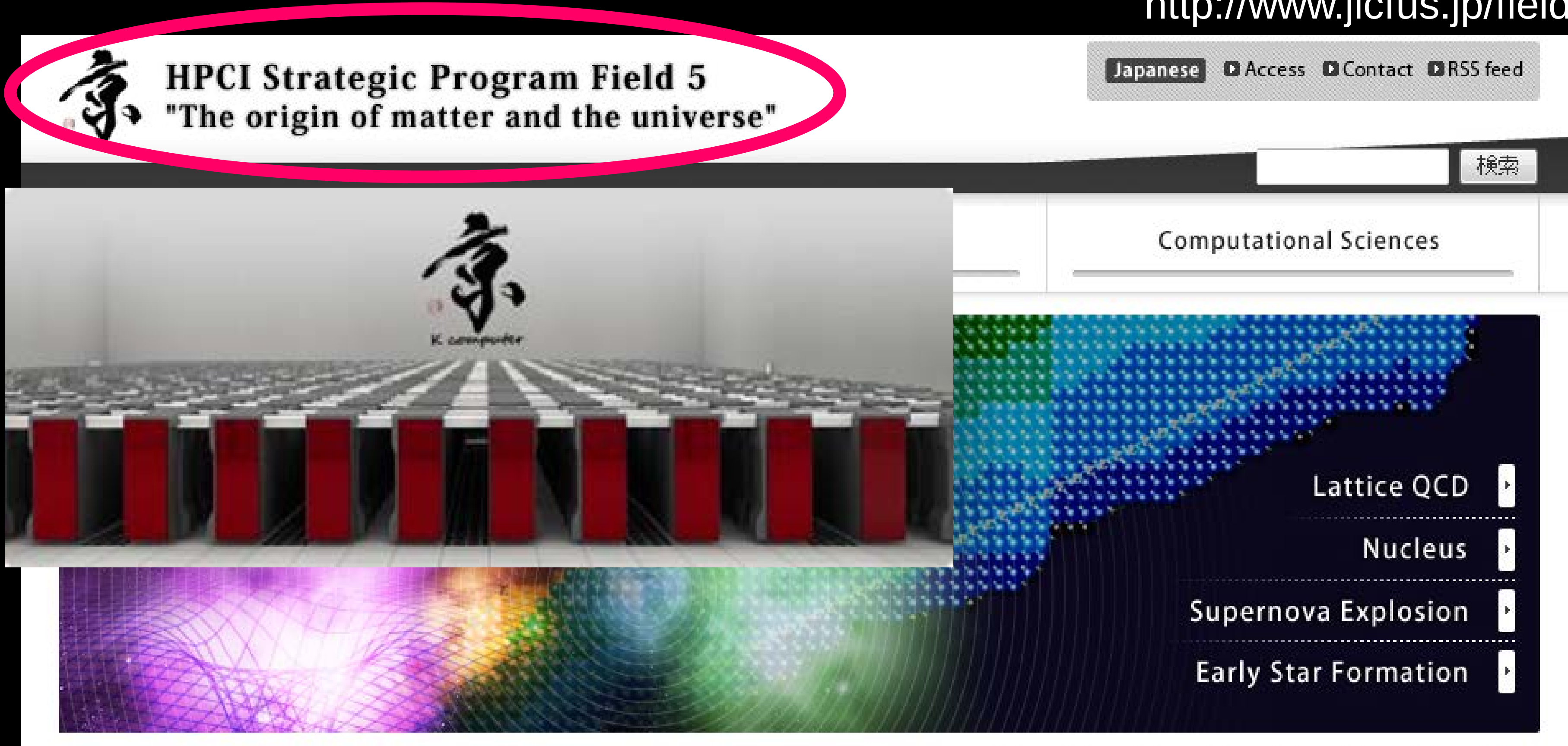

Project 1: Baryon-Baryon interaction from lattice QCD simulations at physical point

Project 2: Large scale quantum many-body calculation of nuclei and its applications

Project 3: Realistic simulation of supernova explosion and black-hole formation

Project 4: Large scale simulation of first generation of stars and galaxies

高密度物質の理解へむけて

1．有限密度格子QCD計算
- 最善の策
- 負符号問題のためμ/T > 1では困難

2．QCDに基づくBB, BBB相互作用 (京コンピューター)
→ 従来の多体問題手法 → ハイペロン物質 with BBB相互作用
- 次善の策： ハイペロンは完全に入る
- 4体力、5体力、...？ クォーク物質への相転移？

3．(低エネルギー) 重イオン衝突実験
- 数倍の原子核密度
- 温度も上がる

4．中性子星観測、マグネター観測
- M-R 関係、冷却曲線： X線、磁場、重力波

5．実験室で類似系（冷却原子分子気体）
- 低密度中性子物質 ⇔ 2成分フェルミ原子気体
- 中間子凝縮 ⇔ 双極フェルミ原子気体
- ハドロン-クォーク相転移 ⇔ 3成分フェルミ原子気体、ボース･フェルミ原子混合気体

Possible Neutron Star Structure

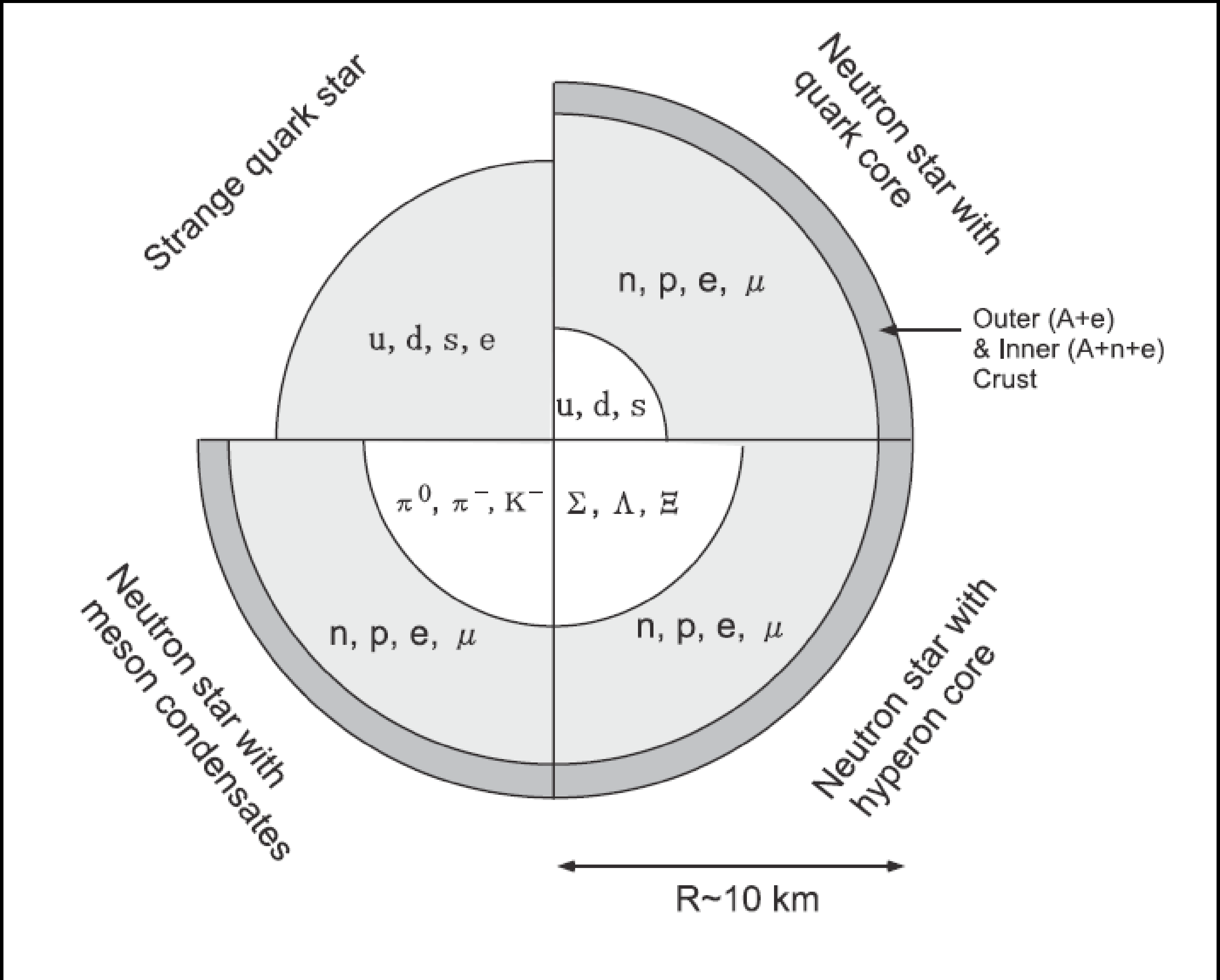

Yagi, Hatsuda and Miake,
"Quark-Gluon Plasma" Cambridge Univ. Press (2008)

Energy per nucleon in pure neutron matter

Morales, (Pandharipande) & Ravenhall, in progress

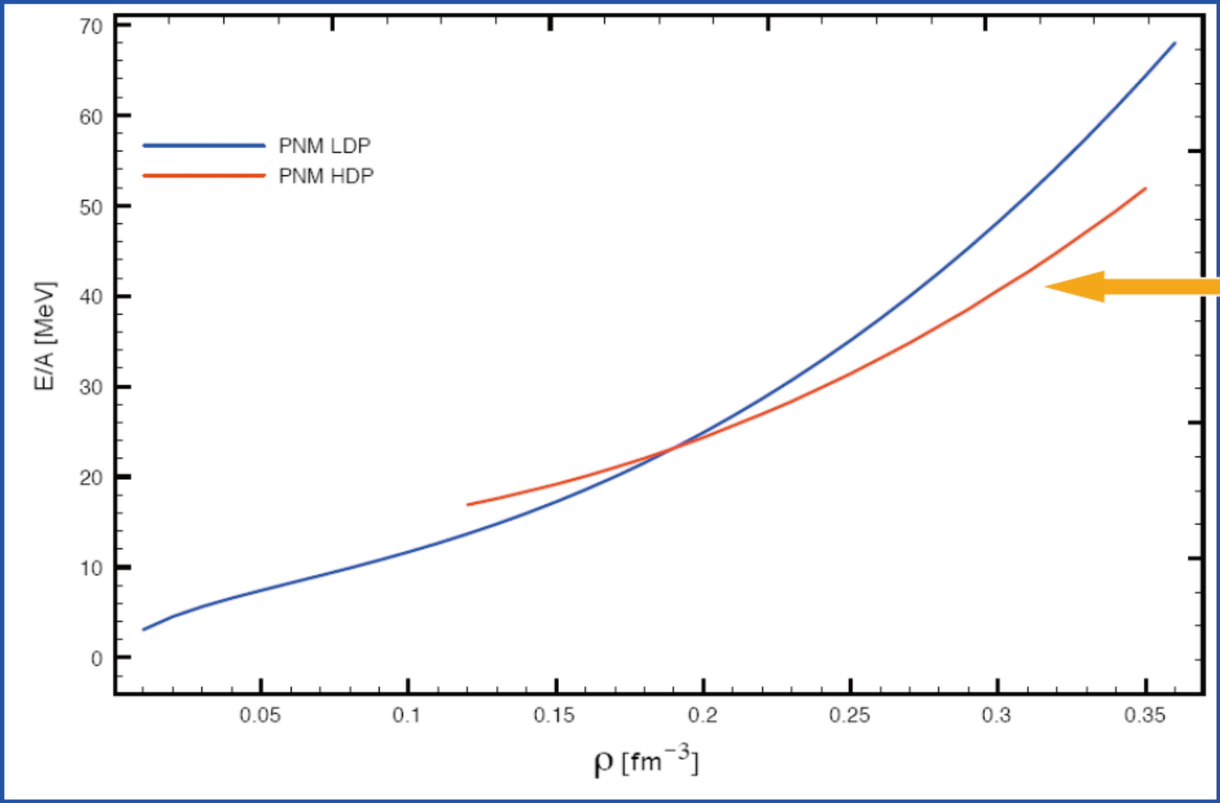

AV-18 + UIV 3-body (IL 3-body too attractive) Improved FHNC algorithms. Two minima!

E/A slightly higher than *Akmal, Pandharipande and Ravenhall, Phys. Rev. C58 (1998) 1804*

Attractive configuration for neutrons (pion-exchange)

$$V_{\mathrm{OPEP}}(r)$$
$$= \frac{f_{\pi N}^2}{4\pi}(\boldsymbol{\tau}_1\cdot\boldsymbol{\tau}_2)(\boldsymbol{\sigma}_1\cdot\nabla_1)(\boldsymbol{\sigma}_2\cdot\nabla_2)\frac{e^{-m_\pi r}}{r}$$
$$= \frac{g_{\pi N}^2}{4\pi}\left(\frac{m_\pi}{2M_N}\right)^2\frac{(\boldsymbol{\tau}_1\cdot\boldsymbol{\tau}_2)}{3}\left[(\boldsymbol{\sigma}_1\cdot\boldsymbol{\sigma}_2)+S_{12}\left(1+\frac{3}{m_\pi r}+\frac{3}{m_\pi^2 r^2}\right)\right]\frac{e^{-m_\pi r}}{r},$$
$$\xrightarrow[\text{chiral limit}]{} \frac{g_A^2}{16\pi F_\pi^2}(\boldsymbol{\tau}_1\cdot\boldsymbol{\tau}_2)\frac{S_{12}}{r^3}$$

$$S_{12} = 3(\boldsymbol{\sigma}_1\cdot\hat{\boldsymbol{r}})(\boldsymbol{\sigma}_2\cdot\hat{\boldsymbol{r}}) - \boldsymbol{\sigma}_1\cdot\boldsymbol{\sigma}_2,$$

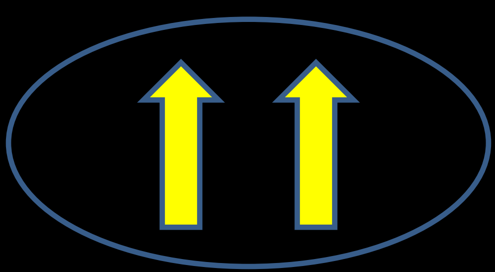
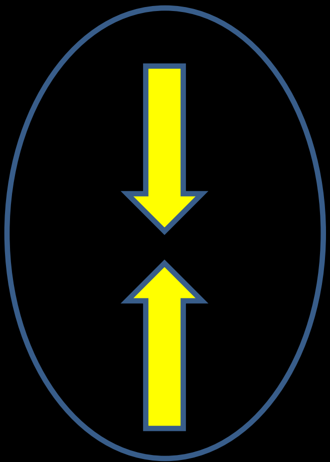
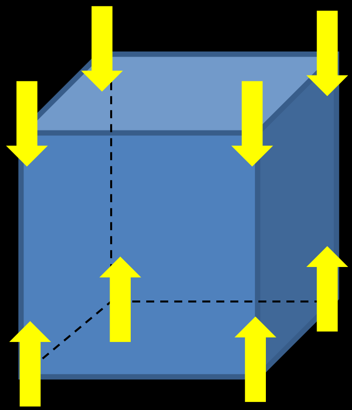

Attractive configuration for neutrons (rho-exchange)

$$V_{\mathrm{OREP}}(r)$$

$$= \frac{f_{\rho N}}{4\pi}(\tau_1 \cdot \tau_2)(\sigma_1 \times \nabla_1)(\sigma_2 \times \nabla_2)\frac{e^{-m_\rho r}}{r}$$

$$= \frac{g_{\rho N}^2}{4\pi}\left(\frac{m_\rho}{2M_N}\right)^2 \frac{\tau_1 \cdot \tau_2}{3}\left[2(\sigma_1 \cdot \sigma_2) - S_{12}\left(1 + \frac{3}{m_\rho r} + \frac{3}{m_\rho^2 r^2}\right)\right]\frac{e^{-m_\rho r}}{r}$$

$$\to -\frac{g_{\rho N}^2}{16\pi M_N^2}(\tau_1 \cdot \tau_2)\frac{S_{12}}{r^3}$$

$$S_{12} = 3(\boldsymbol{\sigma}_1 \cdot \hat{\boldsymbol{r}})(\boldsymbol{\sigma}_2 \cdot \hat{\boldsymbol{r}}) - \boldsymbol{\sigma}_1 \cdot \boldsymbol{\sigma}_2,$$

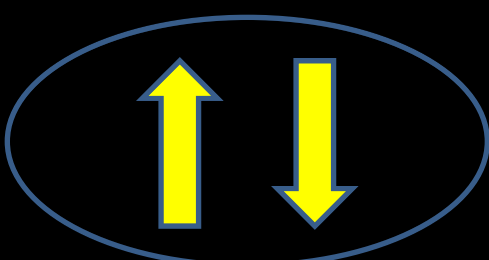

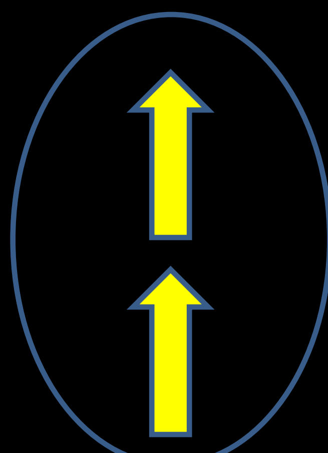

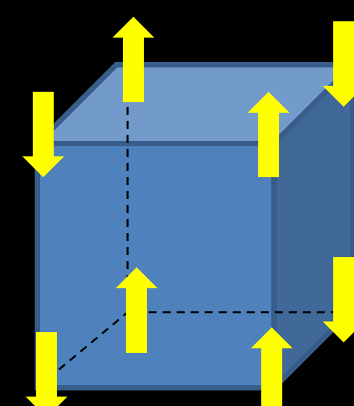

PHYSICAL REVIEW VOLUME 70, NUMBERS 11 AND 12 DECEMBER 1 AND 15, 1946

Theory of Dipole Interaction in Crystals *

J. M. LUTTINGER AND L. TISZA
Research Laboratory of Electronics, Massachusets Institute of Technology, Cambridge, Massachusetts

(Received July 17, 1946)

It is shown that dipole arrays may be represented as vectors in a many-dimensional vector space. The classical dipole interaction energy is a quadratic form in the components of the dipole moments. Its calculation is reduced to the diagonalization of this form. The characteristic vectors are so called basic arrays. An arbitrary array may be decomposed into a linear combination of basic arrays, the energies are additive and may be obtained from the characteristic values of the quadratic form. The method is demonstrated by the complete solution of the characteristic value problem of a highly symmetric class of cubic arrays.. The minimum energy arrays are obtained without and with an external magnetic field for the simple cubic, body-centered cubic, and face-centered cubic lattices. The results are in good qualitative agreement with the experiments of de Haas and Wiersma on Cs Ti alum. Some discrepancies are attributed to quantum effects and to incomplete saturation (entropy $S>0$). The extension to these more general cases will be considered in a following paper.

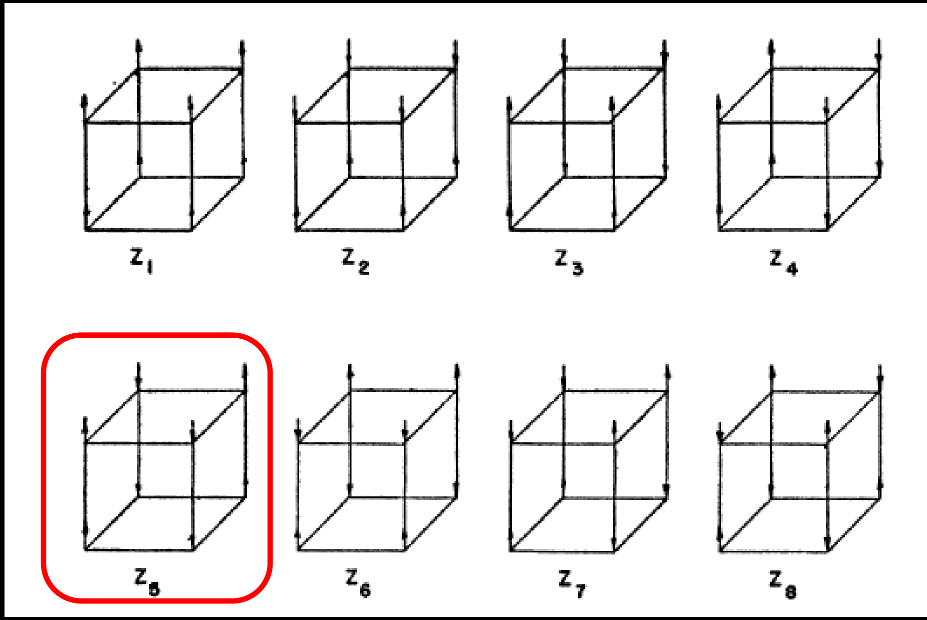

π^0 and/or ρ^0 condensation in neutron matter

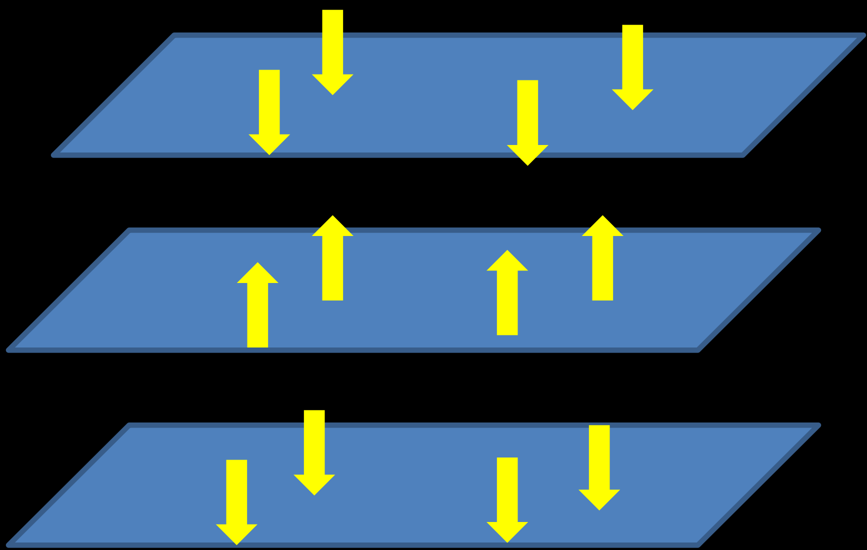

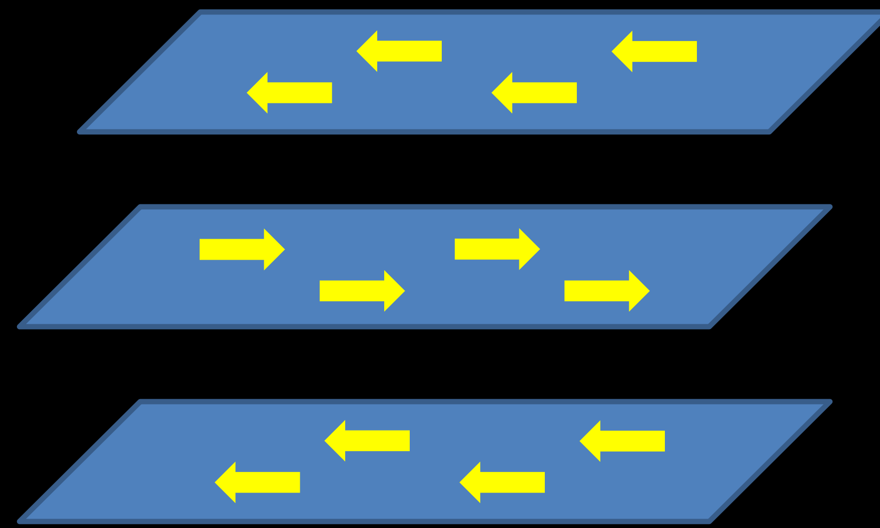

$$(-\nabla^2 + m_\pi^2)\,\varphi_c(\mathbf{r}) = (f/m_\pi)\,\boldsymbol{\nabla}\cdot\langle\psi^\dagger\boldsymbol{\sigma}\psi\rangle$$

$$(-\nabla^2 + m_\rho^2)\,\boldsymbol{\rho}_c(\mathbf{r}) = (f_\rho/m_\rho)\,\boldsymbol{\nabla}\times\langle\psi^\dagger\boldsymbol{\sigma}\psi\rangle$$

A. B. Migdal, NPA (1972)
Takatsuka, Tamagaki & Tatsumi,
Prog. Theor. Phys. Suppl. 112 ('93) 67

Kunihiro, Prog. Theor. Phys. 60 ('78) 1229

π^0 and ρ^0 condensations in neutron matter

E and B condensations in dipolar atoms/molecules

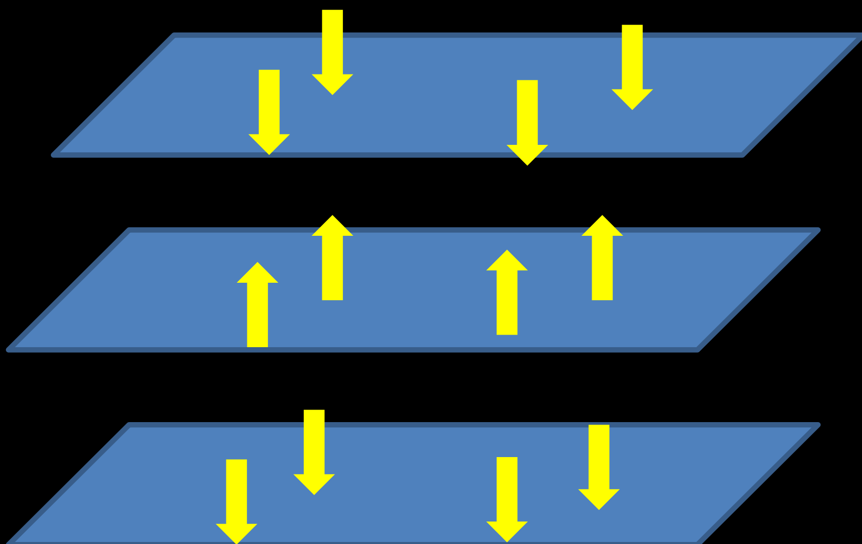

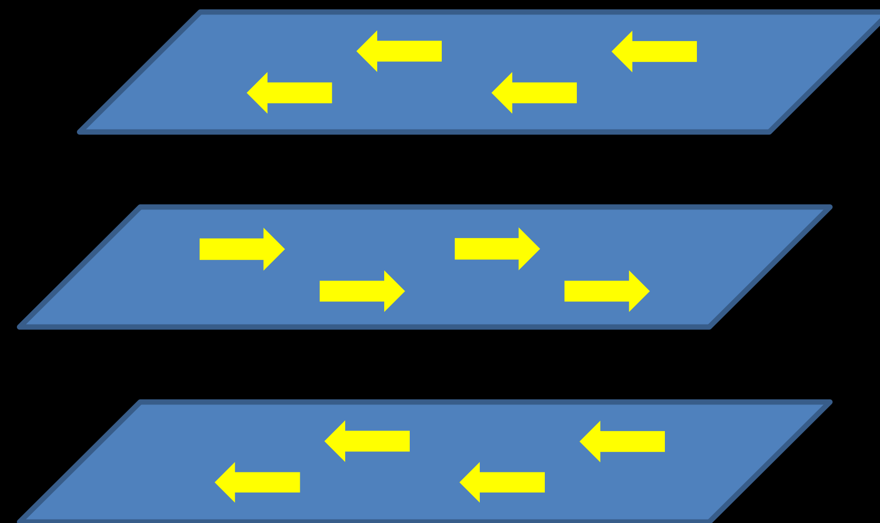

$$(-\nabla^2 + m_\pi^2)\,\varphi_c(\boldsymbol{r}) = (f/m_\pi)\,\boldsymbol{\nabla}\cdot\langle\psi^\dagger\boldsymbol{\sigma}\psi\rangle$$

$$(-\nabla^2 + m_\rho^2)\,\boldsymbol{\rho}_c(\boldsymbol{r}) = (f_\rho/m_\rho)\,\boldsymbol{\nabla}\times\langle\psi^\dagger\boldsymbol{\sigma}\psi\rangle$$

$\varphi \Leftrightarrow A_0$

$-\nabla\varphi \Leftrightarrow E$

$S \Leftrightarrow d$

$\rho \Leftrightarrow A$

$\nabla \times \rho \Leftrightarrow B$

$S \Leftrightarrow \mu$

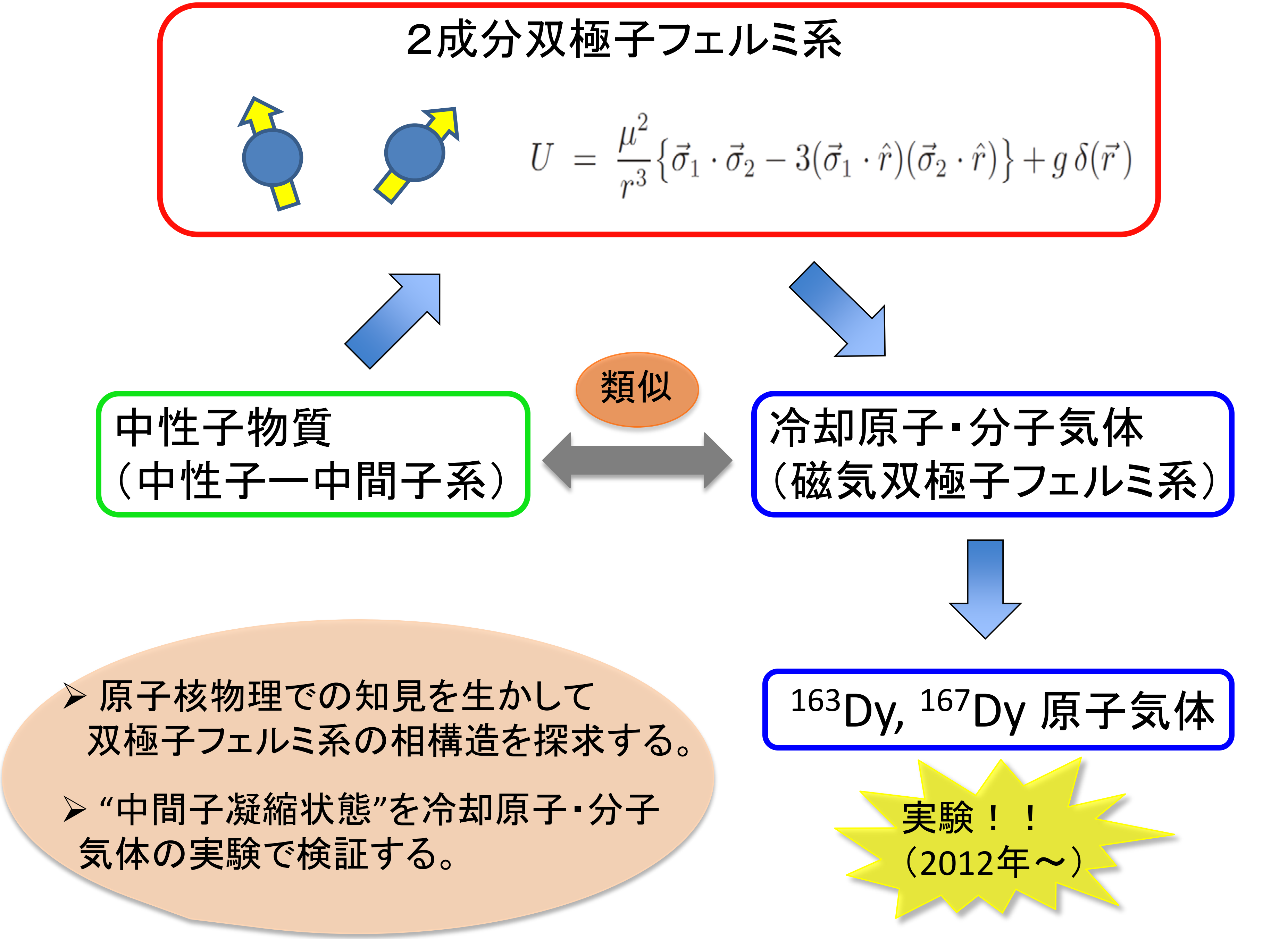

２成分双極子フェルミ系
$U = \frac{\mu^2}{r^3}\{\vec{\sigma}_1\cdot\vec{\sigma}_2 - 3(\vec{\sigma}_1\cdot\hat{r})(\vec{\sigma}_2\cdot\hat{r})\} + g\,\delta(\vec{r})$
類似
中性子物質
（中性子ー中間子系）
冷却原子・分子気体
（磁気双極子フェルミ系）
^{163}Dy, ^{167}Dy 原子気体
実験！！
（2012年～）
➢ 原子核物理での知見を生かして
双極子フェルミ系の相構造を探求する。
➢ “中間子凝縮状態”を冷却原子・分子
気体の実験で検証する。

Ultra-cold atomic Gasses

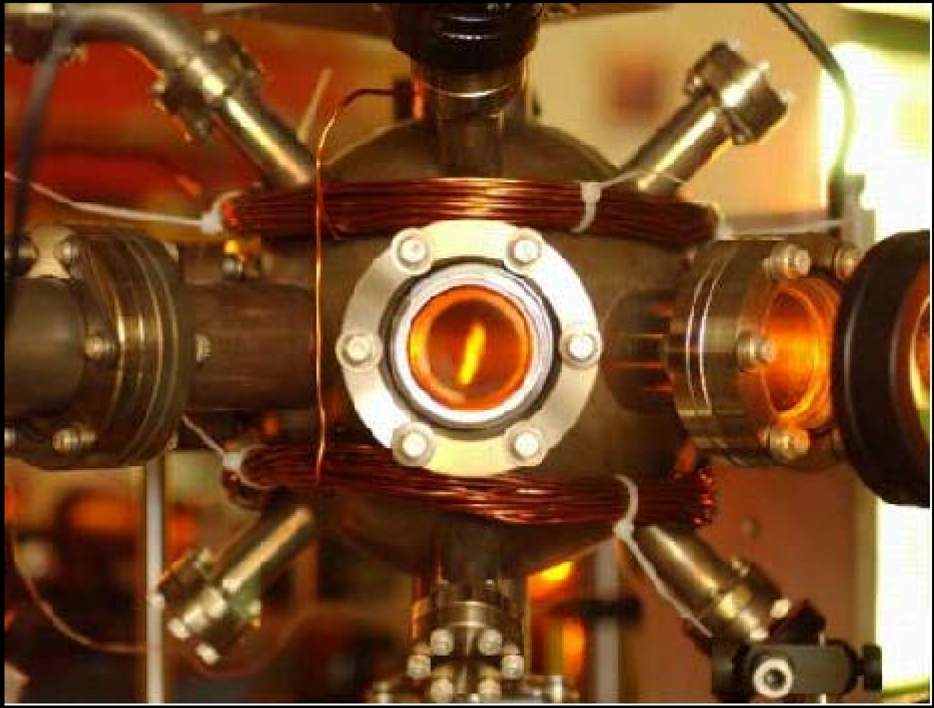

Figure from Pascal Naidon (RIKEN)

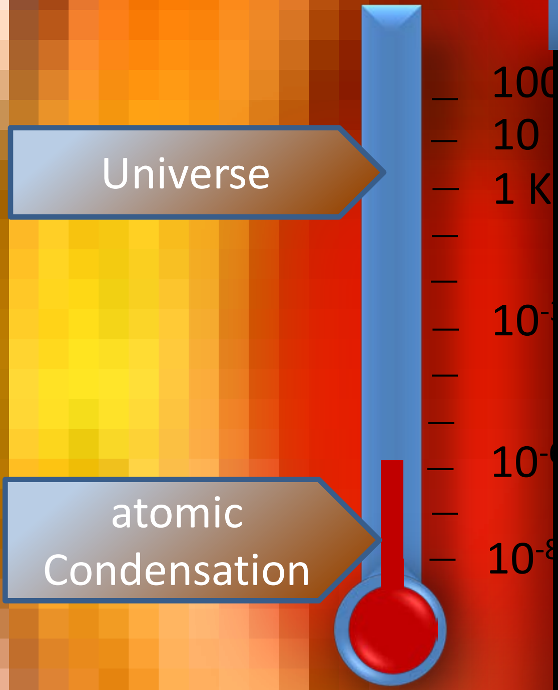

Bose-Einstein Condensate 1995

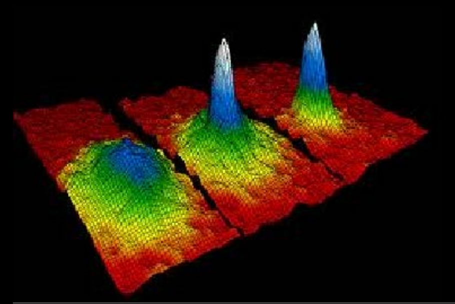

Fermi superfluid 2003

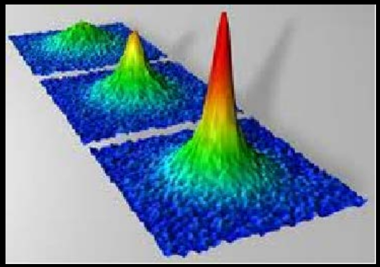

10^{-7} K

QUANTUM FLUIDS (SUPERFLUIDS)

Superfluid helium

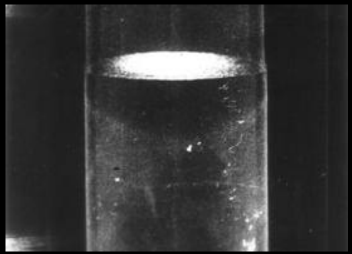

10^{-1} K
1 K

Superconducting electrons

10 K

Superfluid nucleons

Superconducting quarks

10^{9} K

10^{10}K

Physics

Physics **5**, 58 (2012)

Viewpoint

Quantum Dipolar Gases in Boson or Fermion Flavor

Bruno Laburthe-Tolra
Laboratoire de Physique des Lasers, UMR 7538 CNRS, Université Paris 13, 99 Avenue J.-B. Clément, 93430 Villetaneuse, France

Published May 21, 2012

Lanthanide atoms are offering the best opportunities to study the effects of strong dipolar interactions in a quantum gas.

Subject Areas: **Atomic and Molecular Physics**

A Viewpoint on:
Quantum Degenerate Dipolar Fermi Gas
Mingwu Lu, Nathaniel Q. Burdick, and Benjamin L. Lev
Phys. Rev. Lett. **108**, 215301 (2012) – Published May 21, 2012

Bose-Einstein Condensation of Erbium
K. Aikawa, A. Frisch, M. Mark, S. Baier, A. Rietzler, R. Grimm, and F. Ferlaino
Phys. Rev. Lett. **108**, 210401 (2012) – Published May 21, 2012

Physics

Viewpoint

Selected for a Viewpoint in *Physics*
PRL **108,** 210401 (2012) PHYSICAL REVIEW LETTERS week ending 25 MAY 2012

Bose-Einstein Condensation of Erbium

K. Aikawa,[1] A. Frisch,[1] M. Mark,[1] S. Baier,[1] A. Rietzler,[1] R. Grimm,[1,2] and F. Ferlaino[1]

[1]*Institut für Experimentalphysik and Zentrum für Quantenphysik, Universität Innsbruck, Technikerstraße 25, 6020 Innsbruck, Austria*
[2]*Institut für Quantenoptik und Quanteninformation, Österreichische Akademie der Wissenschaften, 6020 Innsbruck, Austria*

(Received 6 April 2012; published 21 May 2012)

s and on the observation of
cooling in an optical dipole
hbach spectroscopy reveals
magnetic-field range up to
o produce a tunable dipolar

37.10.De, 51.60.+a, 67.85.Hj

r interactions

Selected for a Viewpoint in *Physics*
PRL **108,** 215301 (2012) PHYSICAL REVIEW LETTERS week ending 25 MAY 2012

Quantum Degenerate Dipolar Fermi Gas

Mingwu Lu,[1,2,3] Nathaniel Q. Burdick,[1,2,3] and Benjamin L. Lev[2,3,4]

[1]*Department of Physics, University of Illinois at Urbana-Champaign, Urbana, Illinois 61801, USA*
[2]*Department of Applied Physics, Stanford University, Stanford, California 94305, USA*
[3]*E. L. Ginzton Laboratory, Stanford University, Stanford, California 94305, USA*
[4]*Department of Physics, Stanford University, Stanford, California 94305, USA*

(Received 13 March 2012; published 21 May 2012)

We report the first quantum
for exploring strongly correlat
degenerate Fermi gas of the
sympathetically cooling with
factor $T/T_F = 0.2$ below the
to approximately T_c for Bose
dipolar Bose-Fermi gas mixtu
^{161}Dy without ^{162}Dy to T/T_F
of universal dipolar scattering

Bose-Einstein Condensa
K. Aikawa, A. Frisch, M. M
Phys. Rev. Lett. 108, 2104

Meson condensation analogs in ultracold atomic and molecular dipolar gases

Kenji Maeda,[1] Tetsuo Hatsuda,[1,2] and Gordon Baym[3]

[1]*Department of Physics, The University of Tokyo, Tokyo 113-0033, Japan*
[2]*Theoretical Research Division, Nishina Center, RIKEN, Wako 351-0198, Japan*
[3]*Department of Physics, University of Illinois, 1110 W. Green Street, Urbana, Illinois 61801, USA*

We show how an analog of meson condensation in dense nuclear matter can be realized in an ultracold gas of fermionic atoms, or molecules, with large magnetic, or electric, dipole moments. We construct an antiferrosmectic-C phase that at high densities has lower energy than the Fermi gas or ferronematic phases. The antiferrosmectic-C phase is a one-dimensional periodic structure in which the fermions localize in layers with their pseudospin direction aligned parallel to the layers, and staggered layer by layer.

PACS num

arXiv:1205.1086v1 [cond-mat.quant-gas] 5 May 2012

Group → ↓ Period	1	2	3	4	5	6	7	8	9	10	11	12	13	14	15	16	17	18
1	1 H																	2 He
2	3 Li	4 Be											5 B	6 C	7 N	8 O	9 F	10 Ne
3	11 Na	12 Mg											13 Al	14 Si	15 P	16 S	17 Cl	18 Ar
4	19 K	20 Ca	21 Sc	22 Ti	23 V	24 Cr	25 Mn	26 Fe	27 Co	28 Ni	29 Cu	30 Zn	31 Ga	32 Ge	33 As	34 Se	35 Br	36 Kr
5	37 Rb	38 Sr	39 Y	40 Zr	41 Nb	42 Mo	43 Tc	44 Ru	45 Rh	46 Pd	47 Ag	48 Cd	49 In	50 Sn	51 Sb	52 Te	53 I	54 Xe
6	55 Cs	56 Ba	*	72 Hf	73 Ta	74 W	75 Re	76 Os	77 Ir	78 Pt	79 Au	80 Hg	81 Tl	82 Pb	83 Bi	84 Po	85 At	86 Rn
7	87 Fr	88 Ra	**	104 Rf	105 Db	106 Sg	107 Bh	108 Hs	109 Mt	110 Ds	111 Rg	112 Cn	113 Uut	114 Fl	115 Uup	116 Lv	117 Uus	118 Uuo
* Lanthanides			57 La	58 Ce	59 Pr	60 Nd	61 Pm	62 Sm	63 Eu	64 Gd	65 Tb	66 Dy	67 Ho	68 Er	69 Tm	70 Yb	71 Lu	
** Actinides			89 Ac	90 Th	91 Pa	92 U	93 Np	94 Pu	95 Am	96 Cm	97 Bk	98 Cf	99 Es	100 Fm	101 Md	102 No	103 Lr	

Shown above is an 18-column periodic table layout, which has come to be referred to as the common or standard form, on account of its popularity. It is also sometimes referred to as the long form, in comparison to the short Mendeleev-style periodic table. The wide periodic table incorporates the lanthanides and the actinides, rather than separating them from the main body of the table. The extended periodic table adds the 8th and 9th periods, and the theoretical superactinides. The lanthanides and actinides are sometimes instead called the lanthanoids and actinoids.

π^0 and ρ^0 condensations in neutron matter

E and B condensations in dipolar atoms/molecules

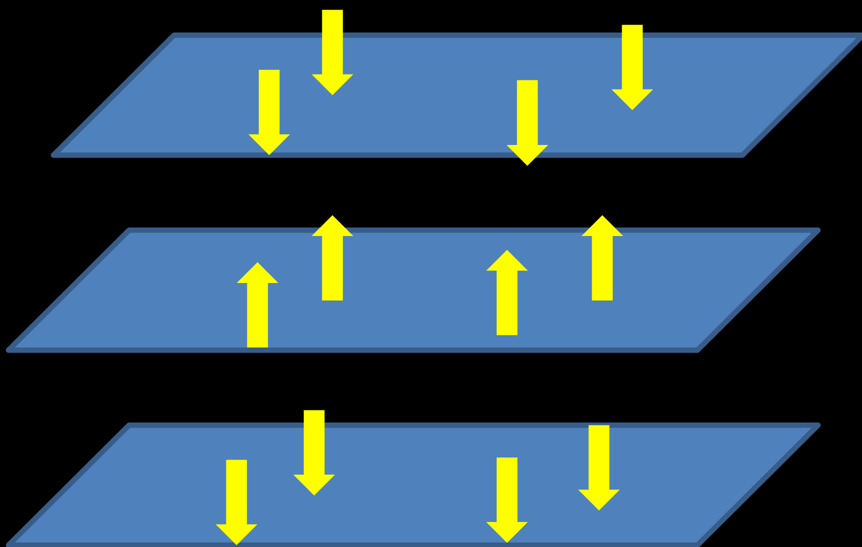

$$(-\nabla^2 + m_\pi^2)\,\varphi_c(\boldsymbol{r}) = (f/m_\pi)\,\boldsymbol{\nabla}\cdot\langle\psi^\dagger\boldsymbol{\sigma}\psi\rangle$$

$\varphi \Leftrightarrow A_0$

$-\nabla\varphi \Leftrightarrow E$

$S \Leftrightarrow d$

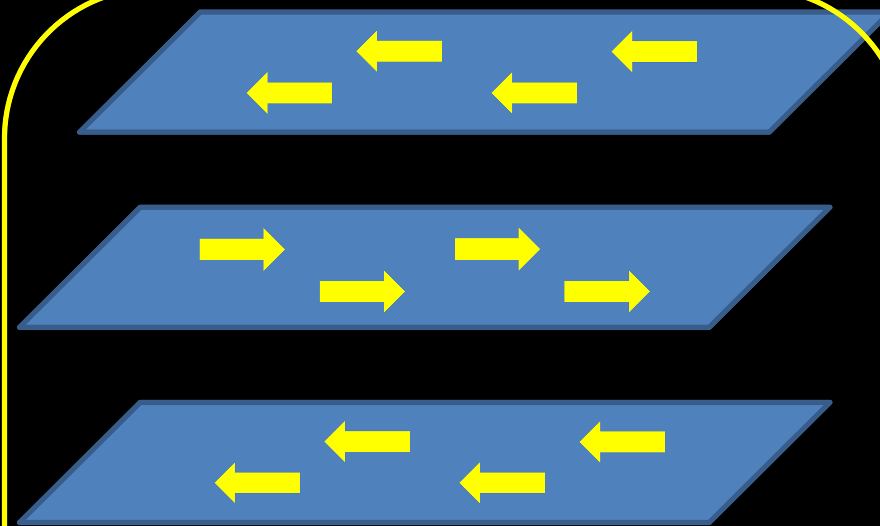

$$(-\nabla^2 + m_\rho^2)\,\boldsymbol{\rho}_c(\boldsymbol{r}) = (f_\rho/m_\rho)\,\boldsymbol{\nabla}\times\langle\psi^\dagger\boldsymbol{\sigma}\psi\rangle$$

$\rho \Leftrightarrow A$

$\nabla x\rho \Leftrightarrow B$

$S \Leftrightarrow \mu$

Two-level model

$$H = \frac{1}{2m}\int d\vec{r}\,\nabla\Psi^\dagger(\vec{r})\cdot\nabla\Psi(\vec{r}) + \frac{1}{8\pi}\int d\vec{r}\,\vec{\mathcal{H}}(\vec{r})^2$$
$$-\mu\int d\vec{r}\,\Psi^\dagger\vec{\sigma}\,\Psi\cdot\vec{\mathcal{H}}(\vec{r}) + g'\int d\vec{r}\,\psi_1^\dagger\psi_2^\dagger\psi_2\psi_1$$

- $\Psi \equiv (\psi_1, \psi_2)^T$: two-component fermions
- $\vec{H}(\vec{r})$: local magnetic field produced by the dipolars
- $\vec{\sigma}$: Pauli matrices

$$\vec{H} = \nabla\times\vec{A}$$

Physical parameters

m : mass , μ : magnetic moment , n : density of atoms

$$n(\vec{r}) = \langle\Psi^\dagger\Psi\rangle,\quad \vec{M}(\vec{r}) = \langle\Psi^\dagger\vec{\sigma}\Psi\rangle,$$

基底状態の候補

1. フェルミ気体状態

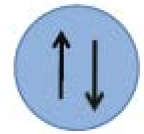

$$|\Phi_{\rm FG}\rangle \;:=\; \prod_{\alpha=\uparrow,\downarrow}\left(\prod_{p\le p_{\rm F}} a^{\dagger}_{\alpha,\vec{p}}\right)|0\rangle$$

2. 偏極フェロネマティック状態

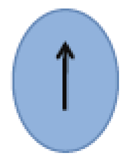

$$|\Phi_{\rm FN}\rangle \;=\; \prod_{\gamma^{-1}(p_x^2+p_y^2)+\gamma^2 p_z^2\le p_{{\rm F},\uparrow}^2} a^{\dagger}_{\uparrow,\vec{p}}\,|0\rangle$$

B.M. Fregoso, E. Fradkin, PRL **103**, 205301 (2009)

3. AFSC状態

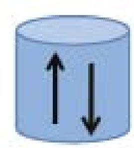

$$|\Phi_{\rm AFSC}\rangle \;=\; \prod_{\ell,\vec{q}_\perp}^{\rm (occ.)} c^{\dagger}_{(\ell,\vec{q}_\perp)}\,|0\rangle$$

Maeda, Hatsuda, Baym, arXiv:1205.1086

	運動エネルギー	近距離斥力	双極子相互作用
1. フェルミ気体状態	控え目	あり	なし
2. 偏極フェロネマティック状態	多い	なし	あり
3. AFSC状態	非常に多い	僅かにあり	あり

AFSC状態 --- 液晶とのアナロジー

液晶

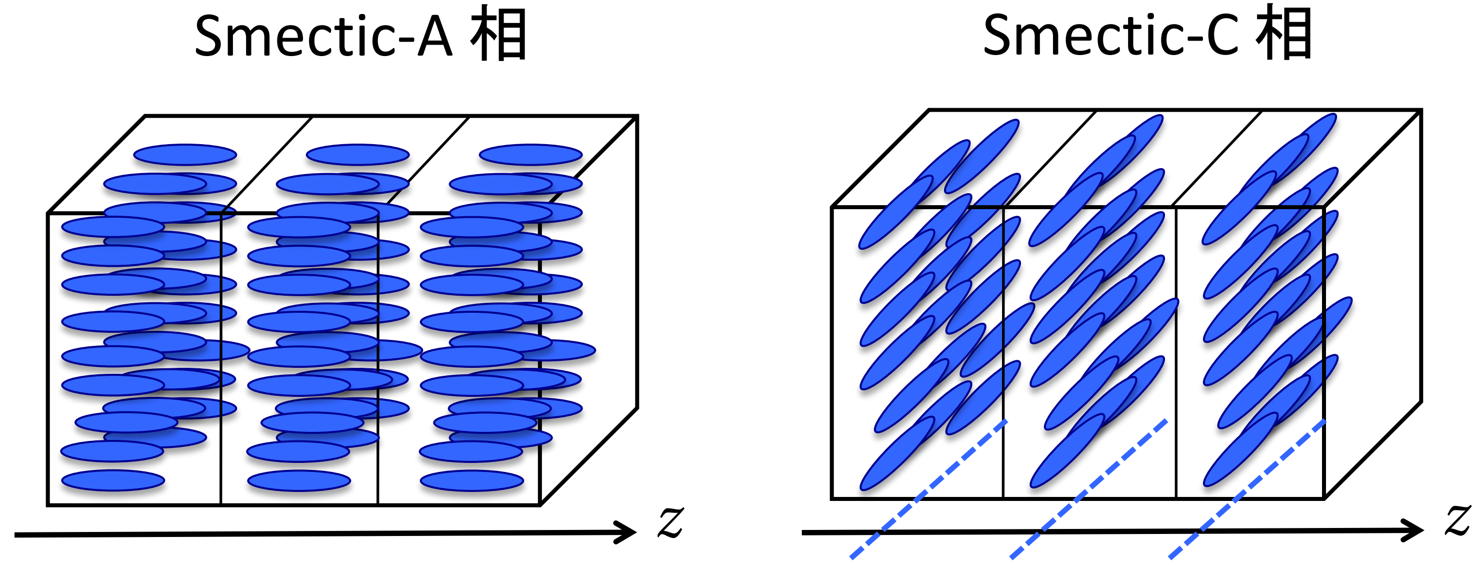

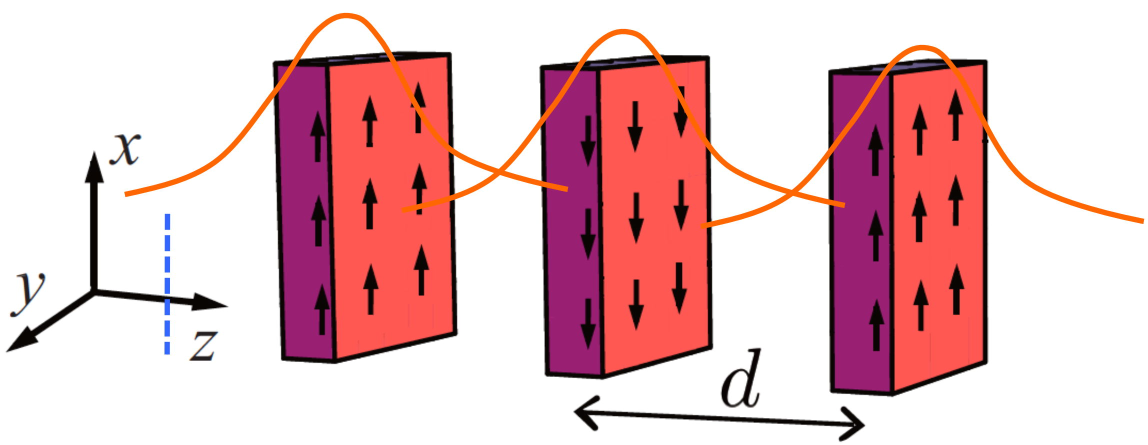

Anti-**F**erro
Smectic-**C** **(AFSC)** state

Maeda, Hatsuda, Baym, arXiv:1205.1086

エネルギー密度--- AFSC状態

$$\tilde{\mathcal{E}}_{\mathrm{AFSC}}$$

$$= \frac{10}{3(3\pi)^{2/3}}\Gamma^{1/3}\alpha^{2/3} + \frac{5}{3(3\pi)^{2/3}}\Gamma^{1/3}\alpha^{-1/3}$$

$$-\frac{20\pi}{3}\lambda_d \sum_{j=1}^{\infty} e^{-(2j-1)^2\pi^2/2\Gamma}\left\{\frac{1}{3} - F(\alpha)\right\}$$

Hartree　Fock

$$+\frac{5}{6}\lambda_s\left\{\frac{1}{2} - \sum_{j=1}^{\infty}\left[e^{-(2j-1)^2\pi^2/2\Gamma} - e^{-2j^2\pi^2/\Gamma}\right]\right\}$$

$Q(\Gamma)$ 僅かな寄与(パウリの排他律による)

運動エネルギー
z方向の零点振動
xy方向の2次元F.E.

双極子ポテンシャル

短距離斥力

競合

変分パラメータ（無次元量）

$$\Gamma = (d/b)^2 \qquad \alpha = 1/(2q_{\mathrm{F}}^2 b^2)$$

相図

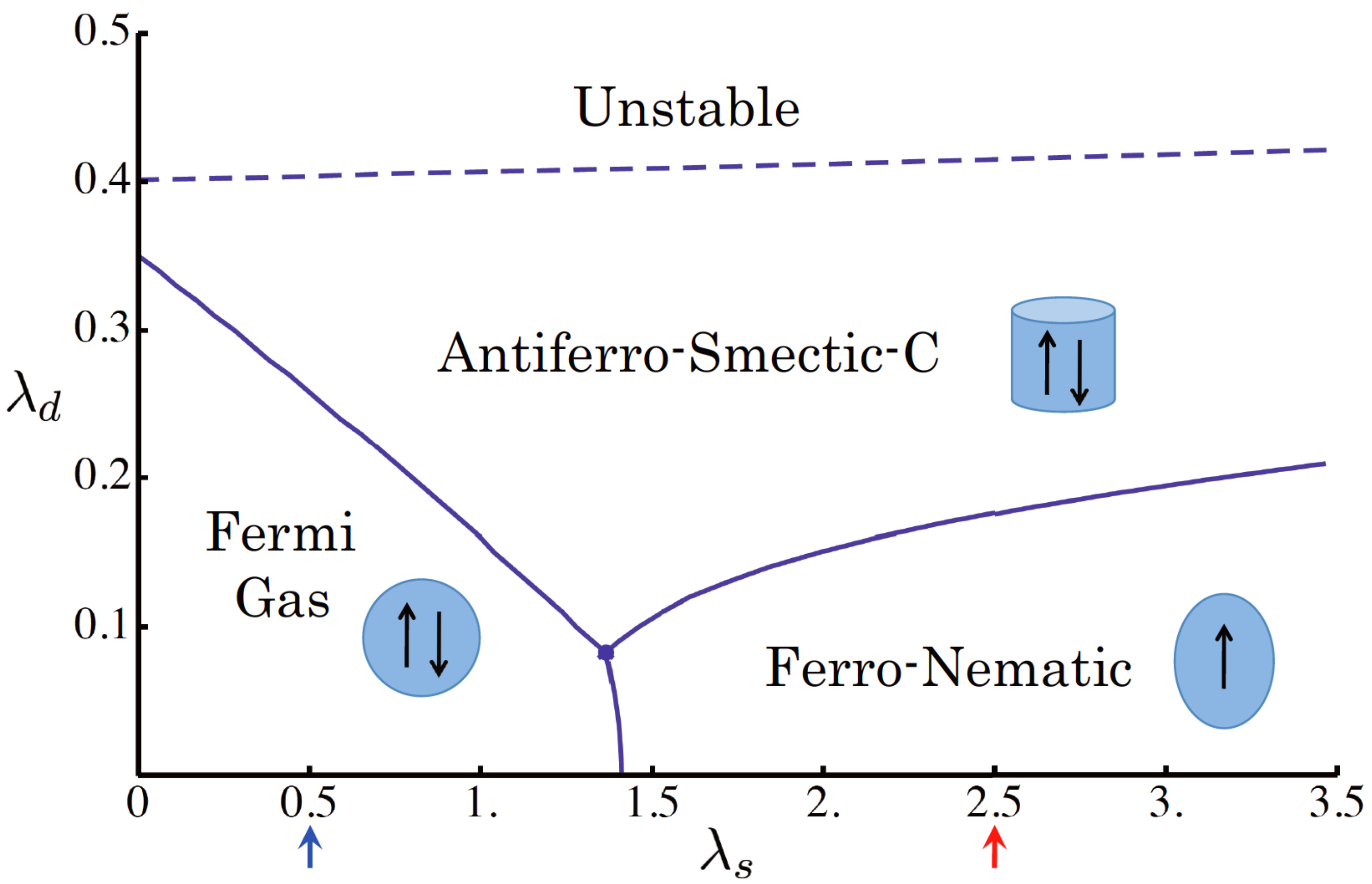
Unstable
Antiferro-Smectic-C
Fermi
Gas
Ferro-Nematic
λ_d
λ_s
0.5
0.4
0.3
0.2
0.1
0
0.5
1.
1.5
2.
2.5
3.
3.5

最近の発展

○　スピン三重項(S=1)励起に対しての
結合チャンネルRPA解析(L=0とL=2の結合)

T. Sogo, M. Urban, P. Shuck, T. Miyakawa ,
PRA **85**, 031601(R) (2012)

フェルミ気体状態は
『空間変調する磁化の発現』に対して不安定である:

$$\left(1-\frac{3}{4}\lambda_s-2\pi\lambda_d\right)\left(1+\frac{\pi}{2}\right)-\frac{\pi^2}{2}\lambda_d^2 \quad = \quad 0$$

○　厳密繰り込み群による不安定性解析

谷崎佑弥　(東大･理) + 初田　in progress

相図--- 最近の発展をふまえて

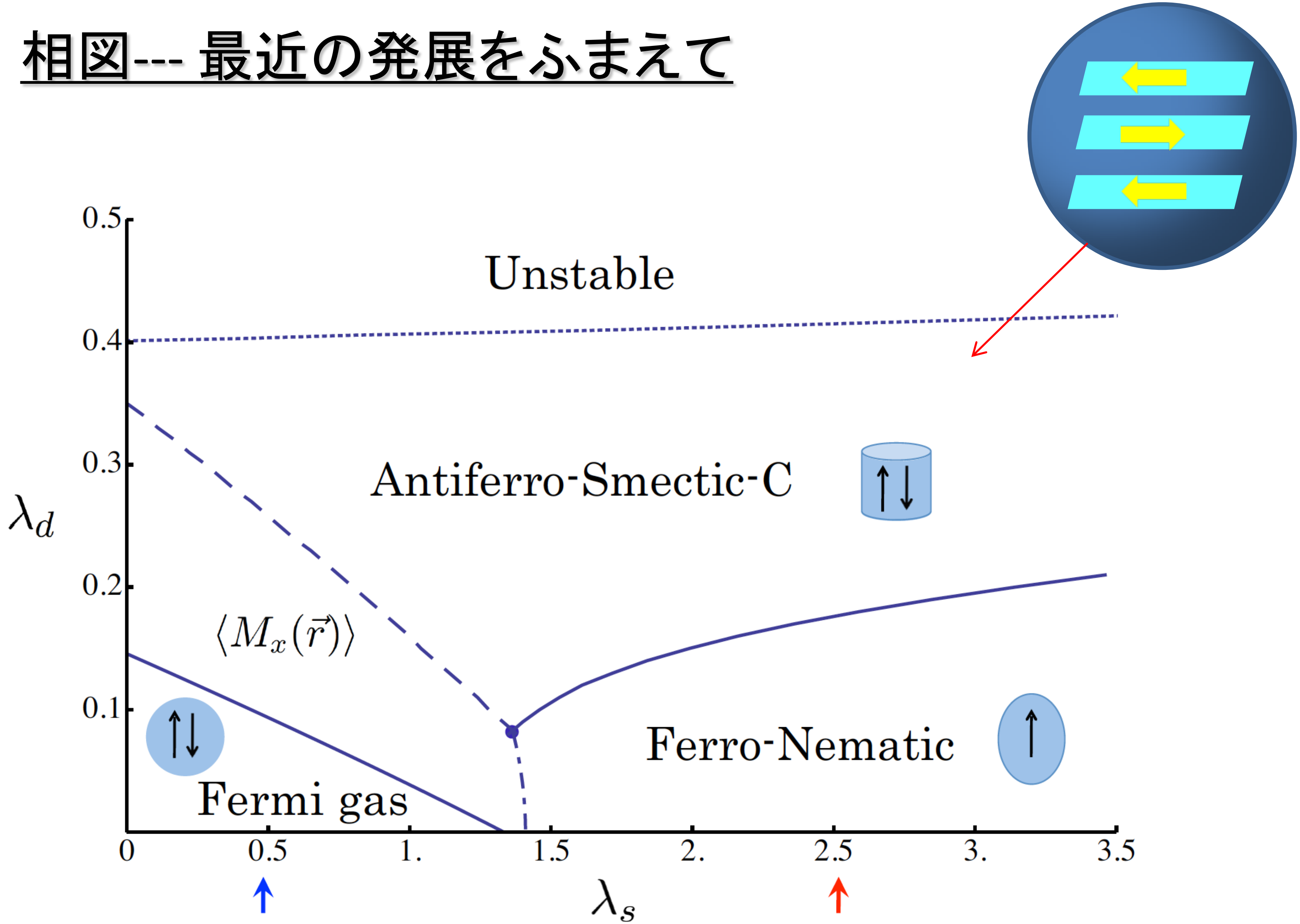

実験との関連

Dy原子、5μB、散乱長10nm

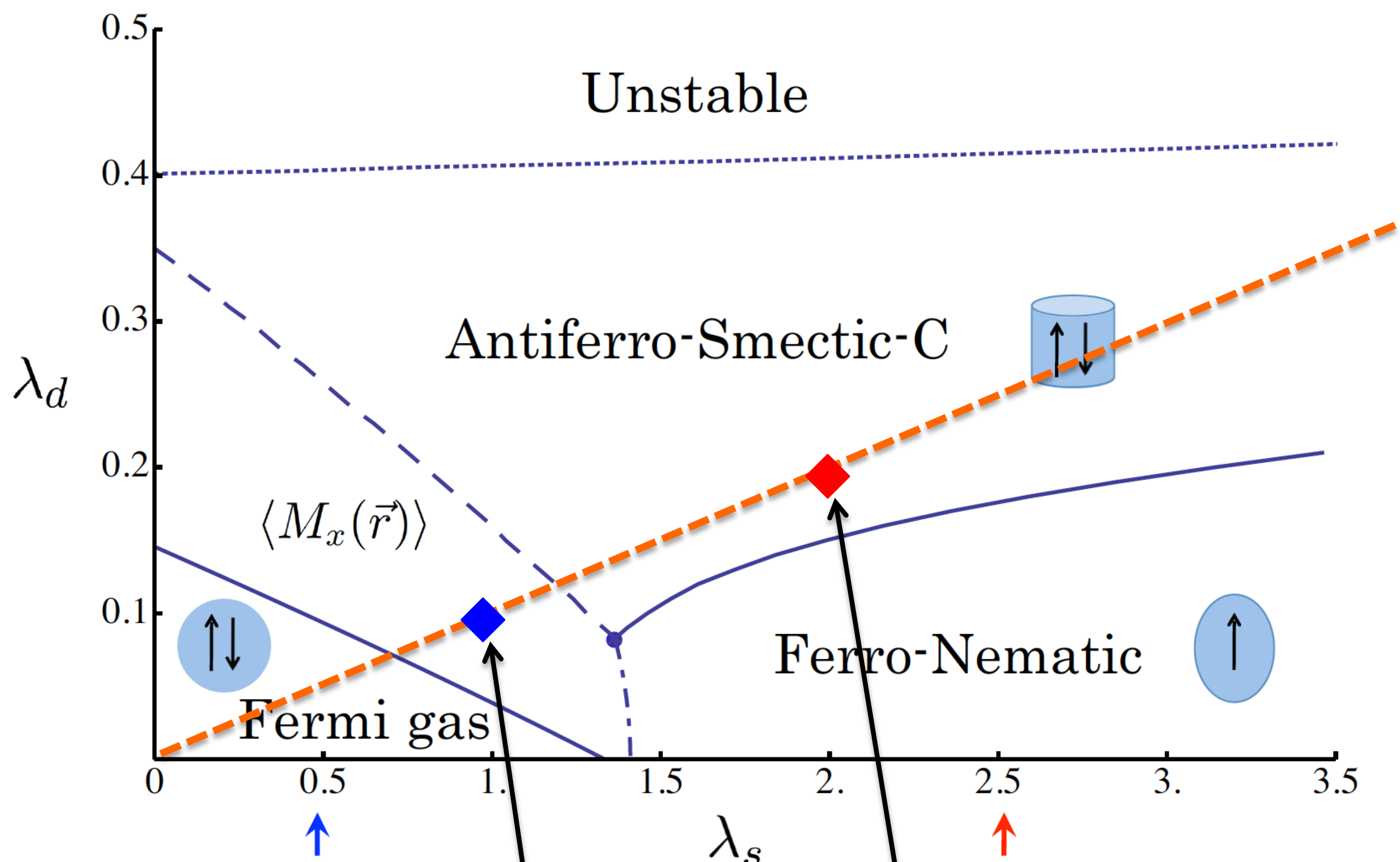

数密度

$7.5*10^{16}$ /cm^3

$6.0*10^{17}$ /cm^3

重力で閉じ込められた中性子 vs. 磁気トラップで閉じ込められたフェルミ原子

Neutron star

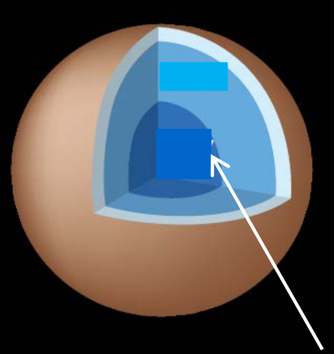

テンソル力による中間子凝縮

cold atoms/molecules

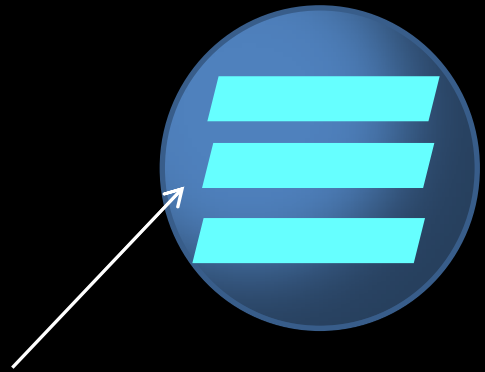

双極型力による光子凝縮

➢ 両者で本質的に同じハミルトニアン

ρ^0 凝縮 ⇔ 磁気双極型冷却フェルミ原子気体のスメクティクC相

ρ^c 凝縮 ⇔ 磁気双極型冷却フェルミ原子気体のコレステリック相？

π^0 凝縮 ⇔ 電気双極型冷却フェルミ原子気体のスメクティクA相？

π^c 凝縮 ⇔ 電気双極型冷却フェルミ原子気体のコレステリック相？

高密度物質の理解へむけて

1．有限密度格子QCD計算
- 最善の策
- 負符号問題のためμ/T > 1では困難

2．QCDに基づくBB, BBB相互作用 (京コンピューター)
→ 従来の多体問題手法 → ハイペロン物質 with BBB相互作用
- 次善の策： ハイペロンは完全に入る
- ４体力、５体力、…？ クォーク物質への相転移？

3．(低エネルギー) 重イオン衝突実験
- 数倍の原子核密度
- 温度も上がる

4．中性子星観測、マグネター観測
- M-R 関係、冷却曲線： X線、磁場、重力波

5．実験室で類似系（冷却原子分子気体）
- 低密度中性子物質 ⇔ 2成分フェルミ原子気体
- 中間子凝縮 ⇔ 双極フェルミ原子気体
- ハドロン-クォーク相転移 ⇔ ３成分フェルミ原子気体、ボース・フェルミ原子混合気体